

The in Vivo Isometric Point of the Lateral Ligament of the Elbow

By Hisao Moritomo, MD, PhD, Tsuyoshi Murase, MD, PhD, Sayuri Arimitsu, MD, Kunihiro Oka, MD, Hideki Yoshikawa, MD, PhD, and Kazuomi Sugamoto, MD, PhD

Investigation performed at the Department of Orthopaedics, Osaka University Graduate School of Medicine, Osaka, Japan

Background: Many reports have discussed reconstruction of the lateral ulnar collateral ligament for the treatment of posterolateral rotatory instability of the elbow, but information regarding the isometric point of the lateral ligament of the elbow is limited. The purposes of the present study were to investigate the in vivo and three-dimensional length changes of the lateral ulnar collateral ligament and the radial collateral ligament during elbow flexion in order to clarify the role of these ligaments as well as to identify the isometric point for the reconstructed lateral ulnar collateral ligament on the humerus where the grafted tendon should be anchored.

Methods: We studied in vivo and three-dimensional kinematics of the normal elbow joint with use of a markerless bone-registration technique. Magnetic resonance images of the right elbows of seven healthy volunteers were acquired in six positions between 0° and 135° of flexion. We created three-dimensional models of the elbow bones, the lateral ulnar collateral ligament, and the radial collateral ligament. The ligament models were based on the shortest calculated paths between each origin and insertion in three-dimensional space with the bone as obstacles. We calculated two types of three-dimensional distances for the ligament paths with each flexion position: (1) between the center of the capitellum and the distal insertions of the ligaments (to investigate the physiological change in ligament length) and (2) between eight different humeral origins and the one typical insertion of the lateral ulnar collateral ligament (to identify the isometric point of the reconstructed lateral ulnar collateral ligament).

Results: The three-dimensional distance for the lateral ulnar collateral ligament was found to increase during elbow flexion, whereas that for the radial collateral ligament changed little. The path of the lateral ulnar collateral ligament gradually developed a detour because of the osseous protrusion of the lateral condyle with flexion. The most isometric point for the reconstructed lateral ulnar collateral ligament was calculated to be at a point 2 mm proximal to the center of the capitellum.

Conclusions: The radial collateral ligament is essentially isometric, but the lateral ulnar collateral ligament is not. The lateral ulnar collateral ligament is loose in elbow extension and becomes tight with elbow flexion.

Clinical Relevance: The present study suggests that the isometric point for the lateral ulnar collateral ligament graft origin is approximately 2 mm proximal to the center of the capitellum.

The function of the lateral ligament of the elbow has been primarily investigated by the application of tensile forces with valgus, varus, or rotational stresses applied to the dissected ligament¹⁻³. The current paradigm that deals with the change of length of the lateral ligament depends almost exclusively on the classic paper by Morrey and An,

which was published in 1985⁴. Those authors investigated the three-dimensional distance between the origin and insertion of the lateral collateral ligament complex and reported that the length of the lateral collateral ligament changed little during elbow flexion. This finding was consistent with the observation that the axis of rotation of the elbow passes through the

Disclosure: In support of their research for or preparation of this work, one or more of the authors received, in any one year, outside funding or grants of less than \$10,000 from Grants-in-Aid for Scientific Research, the Ministry of Education, Science and Culture of Japan. Neither they nor a member of their immediate families received payments or other benefits or a commitment or agreement to provide such benefits from a commercial entity. No commercial entity paid or directed, or agreed to pay or direct, any benefits to any research fund, foundation, division, center, clinical practice, or other charitable or nonprofit organization with which the authors, or a member of their immediate families, are affiliated or associated.

center of the capitellum^{4,6}. However, in that study, Morrey and An did not distinguish the lateral ulnar collateral ligament from the lateral collateral ligament complex. To our knowledge, there have been no reports of studies specifically dealing with the change in length of the lateral ulnar collateral ligament.

Furthermore, all of the current information dealing with the function of the elbow ligaments has been acquired in cadaver studies involving invasive procedures. Such in vitro experiments cannot completely reproduce the muscular force that is exerted across the elbow in vivo. This limitation could alter the normal in vivo kinematics of the ligaments. Recently, researchers have been able to measure in vivo kinematics of the human joint with use of a noninvasive technique^{7,9}, and Marai et al. reported a novel method for calculating ligament length noninvasively in three-dimensional space with bone obstacles (osseous protrusions that deflect a ligament path by ligament-bone impingement)¹⁰.

Posterolateral rotatory instability following disruption of the lateral collateral ligament is the most common form of recurrent posttraumatic instability of the elbow¹¹. It has been theorized that disruption of the lateral ulnar collateral ligament has a crucial role in the development of posterolateral rotatory instability^{11,12}. However, some biomechanical studies

have cast doubt on this theory^{1,3}. Dunning et al., in a study of sequential sectioning of the lateral ulnar elbow ligament, reported that, compared with the intact elbow, no differences in the magnitude of laxity of the ulna were detected with only the radial collateral ligament intact³. Many reports dealing with lateral ulnar collateral ligament reconstruction for the treatment of posterolateral rotatory instability of the elbow have been published¹³⁻¹⁵. In addition, information is limited regarding the in vivo isometric point of the lateral ulnar collateral ligament of the elbow. The purposes of the present study were to investigate the in vivo and three-dimensional length changes of the lateral ulnar collateral ligament and the radial collateral ligament during elbow flexion in order to clarify the role of these ligaments as well as to identify the isometric point for the reconstructed lateral ulnar collateral ligament on the humerus where the grafted tendon should be anchored.

Materials and Methods

We studied the right elbow joints of seven healthy volunteers during elbow flexion with use of a noninvasive, in vivo, three-dimensional motion-analysis system. The patients included five men and two women with a mean age of 28.3 years (range, twenty-four to thirty-three years). All patients consented to be included in the study. The steps in this analysis

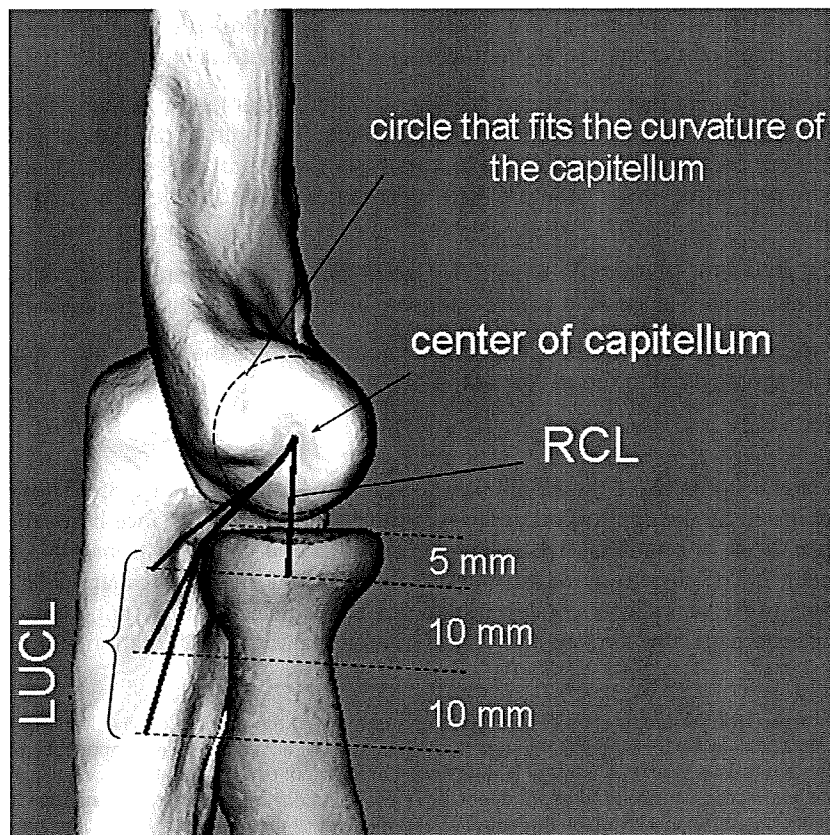


Fig. 1
The paths of the lateral ulnar collateral ligament (LUCL) and the radial collateral ligament (RCL) of the right elbow of a representative case.

included image acquisition, segmentation, and registration. A mathematical description of the motion of the individual bones and their relative motion was derived by computing the rigid transformation required to match the volume data of the models.

Magnetic resonance images of the right elbow of each volunteer were acquired in six positions of elbow flexion (0°, 30°, 60°, 90°, 120°, and 135°) with the same method as was used in our previous study⁷. During this elbow flexion study, the forearm was fixed in the neutral position. Regions of individual bones were semi-automatically segmented from magnetic resonance volume images with use of a software program (Virtual Place-M; AZE, Tokyo, Japan). The software generated three-dimensional surface bone models with use of the marching cubes technique¹⁶. Volume-based registration was done to determine relative positions between volume images represented at different coordinates⁹. Visualization of the geometrical models of each elbow was obtained with a software program that was developed in our laboratory (Orthopedics Viewer; Osaka University, Osaka, Japan).

Ligament Paths

We created three-dimensional models of the ligament paths that approximated the lateral ulnar collateral ligament and the radial collateral ligament. The ligament models were calculated as the shortest paths in three-dimensional space with bone obstacles on the basis of the method proposed by Marai et al.¹⁰. In this program, the paths can be detoured by osseous protrusions to avoid bone penetration. The structural and material properties of the ligaments are not taken into account in this program.

The origins and insertions of the ligament models that are reported in the present study were based solely on the osseous geometry of the elbow. We used anatomical landmarks to identify the origin and insertion points of the ligaments on the bone surfaces.

Normal Length Changes of the Ligaments

We created the ligament paths between the center of the capitellum and the distal insertions of the lateral ulnar collateral ligament

and the radial collateral ligament to investigate the normal length changes of the ligaments. In the present study, the origins of both the lateral ulnar collateral ligament and the radial collateral ligament were located at the center of the capitellum⁴, which was determined as the center of a circle that fit the curvature of the capitellum on the lateral view (Fig. 1). The insertion of the radial collateral ligament was placed at the most lateral point of the radial head at a level 5 mm distal to the proximal surface of the radial head. A previous anatomic study demonstrated that the lateral ulnar collateral ligament and the annular ligament form a broad conjoint insertion measuring approximately 2 cm in width¹⁷. On the basis of that study, three insertion points of the lateral ulnar collateral ligament, located 5, 15, and 25 mm distal to the proximal margin of the radial head, were placed on the supinator crest of the ulna. We calculated the three-dimensional distances of the paths of the lateral ulnar collateral ligament and radial collateral ligament between the origin and insertion of each ligament in six positions of flexion (0°, 30°, 60°, 90°, 120°, and 135°).

Length Changes of the Reconstructed Lateral Ulnar Collateral Ligament

Our goal was to find the isometric point of the reconstructed lateral ulnar collateral ligament at which the ligament's length change would be minimized during elbow flexion. We calculated the length changes of eight possible ligament paths of the reconstructed lateral ulnar collateral ligament on the basis of the eight different humeral origins other than the center of the capitellum and the one typical insertion of the lateral ulnar collateral ligament. The eight different possible origins were defined on the basis of their proximal and anterior locations from the center of the capitellum (Fig. 2, A) and were located at 2-mm intervals. These origins were located on the intersection of a grid whose lines were parallel or perpendicular to the longitudinal axis of the humerus. We first calculated the length changes of each possible ligament path between 0° and 135° of flexion (Figs. 2, B and 2, C) and determined the *most isometric point* of the reconstructed lateral ulnar collateral ligament.

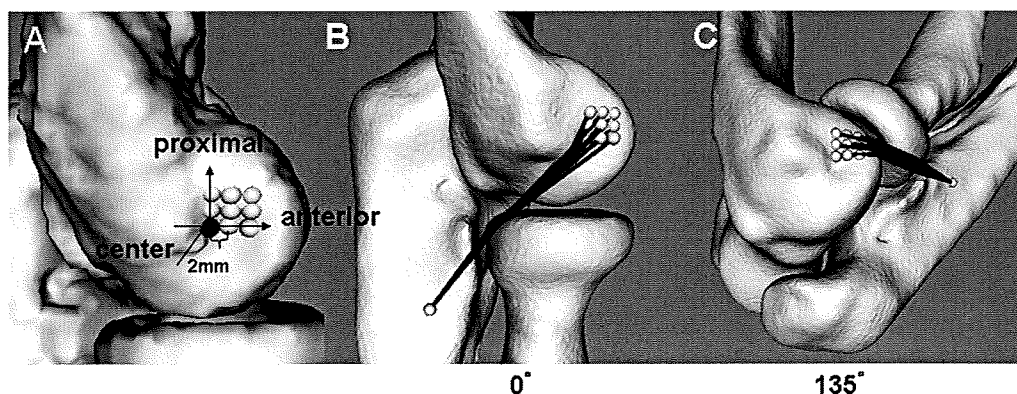


Fig. 2

A: The nine humeral origins of the reconstructed lateral ulnar collateral ligament, separated by 2-mm intervals on the capitellum. B and C: The ligament paths at 0° (B) and 135° of flexion (C) in a representative case.

TABLE I Data on the Ligament Length for Each of the Seven Elbows*

Case	Age (yr)	Gender	Length Change of Normal Ligaments from 0° to 135° of Flexion† (mm)			
			RCL	LUCL-1	LUCL-2	LUCL-3
1	30	M	1.6	2.8	3.0	2.6
2	33	M	1.1	4.0	3.4	2.4
3	25	M	-0.5	4.3	2.2	1.5
4	24	M	0.3	4.0	2.7	2.0
5	25	F	-1.3	2.9	2.5	2.0
6	30	F	0.8	2.8	1.9	1.3
7	31	M	0.1	3.7	2.0	1.2
Average	28.3		0.3	3.5	2.5	1.9
Standard Deviation			1.0	0.7	0.5	0.5

*RCL = radial collateral ligament, and LUCL = lateral ulnar collateral ligament. †The ulnar insertion points of LUCL-1, 2, and 3 are 5, 15, and 25 mm distal to the radial head, respectively. ‡The first value for each humeral origin indicates the anterior distance from the humeral origin to the center of the capitellum, and the second value indicates the proximal distance from the humeral origin to the center of the capitellum.

ament at which the ligament's length change was the smallest. Then, at six flexion positions (0°, 30°, 60°, 90°, 120°, and 135°), we calculated the length change of the reconstructed ligament that had its origin at the isometric point. We defined the insertion point on the ulna to be 15 mm distal from the proximal margin of the radial head.

Statistical Analysis

All data were expressed as the mean and the standard deviation. Statistical analysis of differences was performed with use of the student t test. The level of significance was set at $p < 0.05$. Statistical analysis of differences of the length of

the reconstructed ligament that had its origin at the isometric point was performed with use of repeated-measures analysis of variance.

Results

Normal Length Changes of the Ligaments Lateral Ulnar Collateral Ligament

The three-dimensional animations of the elbow joint showed that all three paths of the lateral ulnar collateral ligament gradually detoured to the lateral side during flexion because of the osseous protrusion of the lateral condyle (Fig. 3). The lateral ulnar collateral ligament was not constrained by the

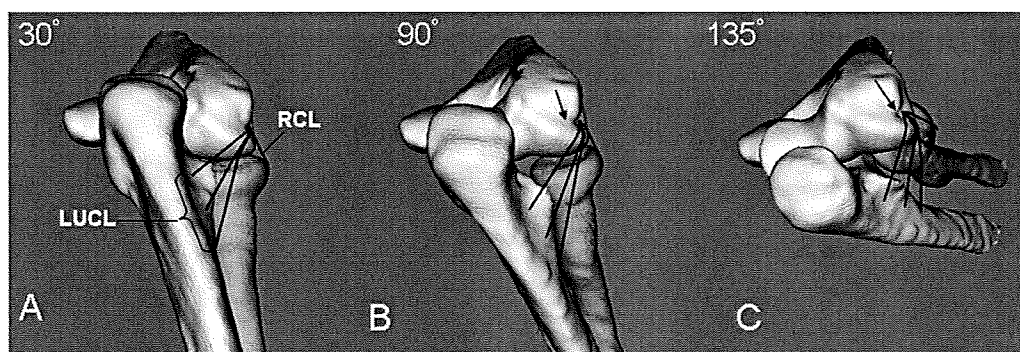


Fig. 3

The ligament paths of the lateral ulnar collateral ligament (LUCL) and the radial collateral ligament (RCL) at 30° (A), 90° (B), and 135° (C) of flexion in a representative case. The right elbows are seen from a posterolateral view. Note that the lateral ulnar collateral ligament paths detour around the osseous protrusion of the lateral condyle at 90° and 135° flexion (arrows).

TABLE I (Continued)

Length Change of Reconstructed LUCL from 0° to 135° of Flexion (mm)									
Humeral Origin†									Average Length of Reconstructed LUCL at 2 mm Proximal to Center and 0 mm Anterior to Center (mm)
Anterior to Center (mm)	0	0	2	2	2	4	4	4	
Proximal to Center (mm)	2	4	0	2	4	0	2	4	
	-0.1	-0.2	-0.6	-4.2	-3.0	-3.8	-4.0	-5.1	43.1 ± 0.9
	-0.1	-1.8	-1.6	-3.0	-4.3	-5.3	-6.3	-7.3	38.6 ± 0.6
	-1.0	-2.3	-2.2	-3.9	-5.2	-5.1	-6.5	-8.3	40.6 ± 0.7
	-1.2	-1.8	-1.6	-2.7	-3.4	-4.2	-3.9	-6.7	38.6 ± 0.7
	-0.3	-2.5	-1.4	-3.1	-4.8	-4.7	-6.1	-7.6	36.1 ± 0.4
	-1.1	-0.3	-1.6	-2.0	-2.9	-4.7	-5.3	-5.7	38.8 ± 0.6
	-1.4	-1.3	-0.1	-0.9	-1.9	-4.0	-3.5	-4.8	39.9 ± 0.8
	-0.7	-1.4	-1.3	-2.8	-3.6	-4.5	-5.1	-6.5	
	0.6	1.0	0.8	1.1	1.2	0.6	1.3	1.3	

lateral condyle in full extension. However, at about 30° of flexion, the lateral ulnar collateral ligament made contact with the posterolateral edge of the lateral condyle at approximately one-fifth of the ligament length on the proximal side of the ligament; then, with further elbow flexion, the lateral ulnar collateral ligament started to detour to the lateral side (Fig. 4) (see Appendix). These findings were true for all seven volunteers in the study.

The three-dimensional distances between the center of the capitellum and the three insertions of the lateral ulnar collateral ligament were found to increase during elbow flexion. The average length change for the three lateral ulnar collateral ligament paths was 2.6 ± 0.9 mm. The increase in length when the insertion point was 5, 15, and 25 mm distal to the radial head was 3.5 ± 0.7 mm, 2.5 ± 0.5 mm, and 1.9 ± 0.5 mm, respectively (Table I).

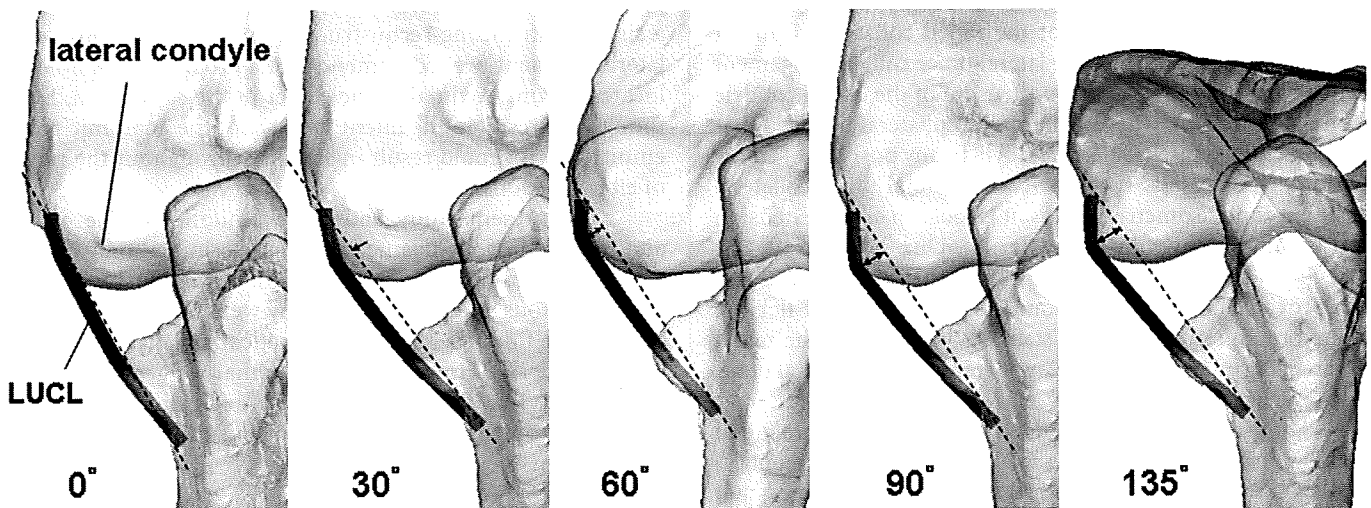


Fig. 4
The typical paths of the lateral ulnar collateral ligament (LUCL) of the right elbow from an anterior view during flexion in a representative case. The ulna is fixed, and the humerus moves; the radius is not seen in these views. Note that, with the elbow flexing, the lateral ulnar collateral ligament paths are gradually detoured by the lateral condyle.

Radial Collateral Ligament

The three-dimensional animations of the elbow joint demonstrated that the radial collateral ligament was not constrained by the lateral condyle in any position of elbow flexion in any of the seven volunteers (Fig. 3). The three-dimensional distance between the center of the capitellum and the radial head increased by 0.3 ± 1.0 mm during flexion (Table I). The increase in the length of the radial collateral ligament was significantly less than that of the lateral ulnar collateral ligament when the insertion point was 5 mm ($p < 0.00005$), 15 mm ($p < 0.0005$), and 25 mm ($p < 0.005$).

Length Changes of the Reconstructed Lateral Ulnar Collateral Ligament

The length changes of the ligament paths for the eight different humeral origins were calculated (Table I). The most isometric point of the reconstructed lateral ulnar collateral ligament was found to be located 2 mm proximal (and 0 mm anterior) to the center of the capitellum; at this point, the average length change was -0.7 ± 0.6 mm. The second most isometric point was 2 mm anterior (and 0 mm proximal) to the center of the capitellum, with an average length change of -1.3 ± 0.8 mm, and the third most isometric point was 4 mm proximal (and 0 mm anterior) to the center of the capitellum, with an average length change of -1.4 ± 1.0 mm. The length of the reconstructed ligament that had its origin at a point 2 mm proximal (and 0 mm anterior) to the capitellar center was constant and did not change significantly through the six elbow flexion positions (Table I).

Discussion

In the present study, the three-dimensional distance of the lateral ulnar collateral ligament, which was defined as the distance between the center of the capitellum and the supinator crest of the ulna, was found to increase gradually during elbow flexion, whereas that of the radial collateral ligament changed little. The path of the lateral ulnar collateral ligament detoured around the osseous protrusion of the lateral condyle with elbow flexion, whereas the radial collateral ligament was not constrained by the lateral condyle in any position of elbow flexion. These results suggest that the lateral ulnar collateral ligament is not isometric; that is, it is loose in elbow extension and becomes tight with elbow flexion. Our data also suggest that the radial collateral ligament is essentially isometric and can provide stability throughout the range of elbow flexion. Therefore, in terms of elbow stability, we consider the radial collateral ligament to be more important than the lateral ulnar collateral ligament.

Some authors have attributed the cause of posterolateral rotatory instability to the lateral ulnar collateral ligament^{11,12}. However, some recent anatomical studies have indicated that more than half of the cadavers lacked an obvious and thick lateral ulnar collateral ligament¹⁸. Also, some biomechanical studies have shown that the lateral ulnar collateral ligament can be transected without inducing posterolateral rotatory in-


stability of the elbow¹⁻³. The results of the present in vivo study are in agreement with those findings, which cast doubt on the theory that the lateral ulnar collateral ligament is crucial to elbow stability. We speculate that the lateral ulnar collateral ligament may be a secondary stabilizer of the lateral collateral ligamentous complex.

Nevertheless, the lateral ulnar collateral ligament reconstruction procedure that is performed for the treatment of posterolateral rotatory instability has been reported to be a successful and effective procedure¹³⁻¹⁵. At the time of the ligament reconstruction, knowledge of the isometric point of the lateral ulnar collateral ligament is important because stability throughout the range of elbow motion cannot be achieved without the reconstructed ligaments being fixed to the isometric point. The isometric point of the lateral ulnar collateral ligament has been thought to be identical to the axis of rotation and to be located at the center of the capitellum, and, therefore, clinically, a drill-hole has been placed at that location^{14,15}. However, on several occasions, we have found during surgery that the reconstructed ligament became loose upon elbow extension whereas it was tight with elbow flexion. Therefore, we have often added a side-to-side suture for the reconstructed lateral ulnar collateral ligament to the remnant of the radial collateral ligament and the annular ligament. Doing so bends the path of the lateral ulnar collateral ligament slightly anteriorly, which approximates its path to being almost the same as that of the normal course of the radial collateral ligament and the annular ligament. This bending of the reconstructed ligament anteriorly may be one reason why this type of lateral ulnar collateral ligament reconstruction has been reported to be successful and effective.

In the present study, we found that the isometric point of the reconstructed lateral ulnar collateral ligament was not located at the center of the capitellum but was located 2 mm proximal to it. Therefore, to obtain more stability with use of a single graft during reconstruction of the lateral ulnar collateral ligament, we recommend that a proximal drill hole be located 2 mm proximal to the center of the capitellum. Even though the resultant ligament path is not the anatomic path, empirically it should result in stability throughout the range of elbow flexion.

The present study had some limitations. The origin and insertion of the ligaments were determined only on the basis of general anatomic information; individual variances in ligamentous and skeletal anatomy were not taken into account. Our findings are only theoretical and have not been tested surgically. However, the paths that we generated provide useful visual information about the ligaments and help to identify potential joint mobility constraints imposed by the ligaments.

Appendix

 A video demonstrating the course of the simulated lateral ulnar collateral ligament with elbow motion is available with the electronic versions of this article, on our

web site at jbjs.org (go to the article citation and click on “Supplementary Material”) and on our quarterly CD-ROM (call our subscription department, at 781-449-9780, to order the CD-ROM). ■

NOTE: The authors thank Takehiro Arimura, RT, of the Department of Radiology, and Ryoji Nakao, MEng, of the Department of Orthopaedics, Osaka University Graduate School of Medicine, for their assistance during parts of the experimental procedures.

Hisao Moritomo, MD, PhD
Tsuyoshi Murase, MD, PhD
Sayuri Arimitsu, MD
Kunihiko Oka, MD
Hideki Yoshikawa, MD, PhD
Kazuomi Sugamoto, MD, PhD
Department of Orthopaedic Surgery, Osaka University, 2-2 Yamadaoka, Suita-shi, Osaka 565-0871, Japan

References

1. Olsen BS, Sojbjerg JO, Dalstra M, Sneppen O. Kinematics of the lateral ligamentous constraints of the elbow joint. *J Shoulder Elbow Surg.* 1996;5:333-41.
2. Olsen BS, Sojbjerg JO, Nielsen KK, Vaesel MT, Dalstra M, Sneppen O. Posterolateral elbow joint instability: the basic kinematics. *J Shoulder Elbow Surg.* 1998;7:19-29.
3. Dunning CE, Zarzour ZD, Patterson SD, Johnson JA, King GJ. Ligamentous stabilizers against posterolateral rotatory instability of the elbow. *J Bone Joint Surg Am.* 2001;83:1823-8.
4. Morrey BF, An KN. Functional anatomy of the ligaments of the elbow. *Clin Orthop Relat Res.* 1985;201:84-90.
5. London JT. Kinematics of the elbow. *J Bone Joint Surg Am.* 1981;63:529-35.
6. Deland JT, Garg A, Walker PS. Biomechanical basis for elbow hinge-distractor design. *Clin Orthop Relat Res.* 1987;215:303-12.
7. Goto A, Moritomo H, Murase T, Oka K, Sugamoto K, Arimura T, Nakajima Y, Yamazaki T, Sato Y, Tamura S, Yoshikawa H, Ochi T. In vivo elbow biomechanical analysis during flexion: three-dimensional motion analysis using magnetic resonance imaging. *J Shoulder Elbow Surg.* 2004;13:441-7.
8. Crisco JJ, Coburn JC, Moore DC, Akelman E, Weiss AP, Wolfe SW. In vivo radiocarpal kinematics and the dart thrower's motion. *J Bone Joint Surg Am.* 2005;87:2729-40.
9. Moritomo H, Murase T, Goto A, Oka K, Sugamoto K, Yoshikawa H. In vivo three-dimensional kinematics of the midcarpal joint of the wrist. *J Bone Joint Surg Am.* 2006;88:611-21.
10. Marai GE, Laidlaw DH, Demiralp Ç, Andrews S, Grimm CM, Crisco JJ. Estimating joint contact areas and ligament lengths from bone kinematics and surfaces. *IEEE Trans Biomed Eng.* 2004;51:790-9.
11. O'Driscoll SW. Classification and evaluation of recurrent instability of the elbow. *Clin Orthop Relat Res.* 2000;370:34-43.
12. O'Driscoll SW, Bell DF, Morrey BF. Posterolateral rotatory instability of the elbow. *J Bone Joint Surg Am.* 1991;73:440-6.
13. Nestor BJ, O'Driscoll SW, Morrey BF. Ligamentous reconstruction for posterolateral rotatory instability of the elbow. *J Bone Joint Surg Am.* 1992;74:1235-41.
14. Olsen BS, Sojbjerg JO. The treatment of recurrent posterolateral instability of the elbow. *J Bone Joint Surg Br.* 2003;85:342-6.
15. Lee B, Teo LH. Surgical reconstruction for posterolateral rotatory instability of the elbow. *J Shoulder Elbow Surg.* 2003;12:476-9.
16. Lorensen WE, Cline HE. Marching cubes: a high resolution 3D surface construction algorithm. *ACM SIGGRAPH Comput Graph.* 1987;21:163-9.
17. Cohen MS, Hastings H 2nd. Rotatory instability of the elbow. The anatomy and role of the lateral stabilizers. *J Bone Joint Surg Am.* 1997;79:225-33.
18. Takahashi K, Minami A, Kato H, Kasajima T, Hirachi K. Anatomical study of lateral ligament complex of the elbow. *J Jpn Elbow Soc.* 1997;4:15-6.

A three-dimensional quantitative analysis of carpal deformity in rheumatoid wrists

S. Arimitsu,
T. Murase,
J. Hashimoto,
K. Oka,
K. Sugamoto,
H. Yoshikawa,
H. Moritomo

From Osaka
University Graduate
School of Medicine,
Osaka, Japan

We have measured the three-dimensional patterns of carpal deformity in 20 wrists in 20 rheumatoid patients in which the carpal bones were shifted ulnarwards on plain radiography. Three-dimensional bone models of the carpus and radius were created by computerised tomography with the wrist in the neutral position. The location of the centroids and rotational angle of each carpal bone relative to the radius were calculated and compared with those of ten normal wrists.

In the radiocarpal joint, the proximal row was flexed and the centroids of all carpal bones translocated in an ulnar, proximal and volar direction with loss of congruity. In the midcarpal joint, the distal row was extended and congruity generally well preserved. These findings may facilitate more positive use of radiocarpal fusion alone for the deformed rheumatoid wrist.

The most common deformity of the wrist in rheumatoid arthritis (RA) has been described as carpal supination with ulnar translocation¹ and many reports have attempted to evaluate this deformity.²⁻⁸ However, they have been two-dimensional studies based generally on radiological assessment, the value of which is limited because the complex, overlapping appearance makes measurement difficult, especially in wrists with severe deformity. We have therefore undertaken an analysis of such deformities using a new three-dimensional (3D) technique.

Patients and Methods

We studied 20 wrists in 20 rheumatoid patients in which there was ulnar translocation on the anteroposterior radiograph. We chose wrists with a carpal-ulnar distance ratio below 0.27⁹ and in which the shape of each bone was easily recognisable (Fig. 1). There were 19 women and one man with a mean age of 61 years (21 to 80). The mean duration of the disease was 15 years (6 to 38). A total of 18 patients had the more erosive subset of the disease, one the least erosive¹⁰ and one juvenile RA. For comparison, we also chose a control group of ten normal wrists in ten men with a mean age of 41.4 years (18 to 76).

Imaging. Computerised tomography (CT) with a slice thickness of 0.625 mm was undertaken on a clinical helical-type scanner (LightSpeed Ultra16; General Electric, Maukesha,

Wisconsin). During image acquisition, the wrists were in the neutral position with the axes of the third metacarpal and forearm aligned. The data were saved in a standard format (DICOM; Digital Imaging and Communications in Medicine).

Segmentation and construction of three-dimensional surface bone models. Segmentation is the extraction of individual bony regions. The anatomy or region of interest must be delineated and separated so that it can be viewed individually and 3D models reconstructed. Regions of individual bones were segmented semi-automatically using a software program for image analysis (Virtual Place-M; AZE Ltd, Tokyo, Japan). Surface models of the radius and each carpal bone were obtained by 3D surface generation of the bone cortex.¹¹⁻¹³

Measurement of centroid translocation and carpal rotation. First, the position of the volume centroid of any bone was calculated from the CT files.¹⁴ In order to measure the translocation, we defined the grid for the lower radius and each carpal bone within it. This was the orthogonal reference system originally advocated by Belsole et al¹⁵ (Figs 2 and 3). For the radius this was determined as follows: The Y axis was the longitudinal radial axis and indicated the proximal (+)/distal (-) direction; the Z axis was the line through the styloid perpendicular to the Y axis and indicated radial (+)/ulnar (-) displacement; the X axis was the

■ S. Arimitsu, MD, Orthopaedic Surgeon
■ T. Murase, MD, PhD, Assistant Professor
■ J. Hashimoto, MD, PhD, Associate Professor
■ K. Oka, MD, Orthopaedic Surgeon
■ K. Sugamoto, MD, PhD, Professor
■ H. Yoshikawa, MD, PhD, Professor
■ H. Moritomo, MD, PhD, Assistant Professor
Department of Orthopaedic Surgery
Osaka University Graduate School of Medicine, 2-2, Yamada-oka, Suita, Osaka 565-0871, Japan.

Correspondence should be sent to Dr S. Arimitsu; e-mail: sayu@df6.so-net.ne.jp

©2007 British Editorial Society of Bone and Joint Surgery
doi:10.1302/0301-620X.89B4.18476 \$2.00

J Bone Joint Surg [Br]
2007;89-B:490-4.
Received 31 July 2006;
Accepted after revision
5 December 2006

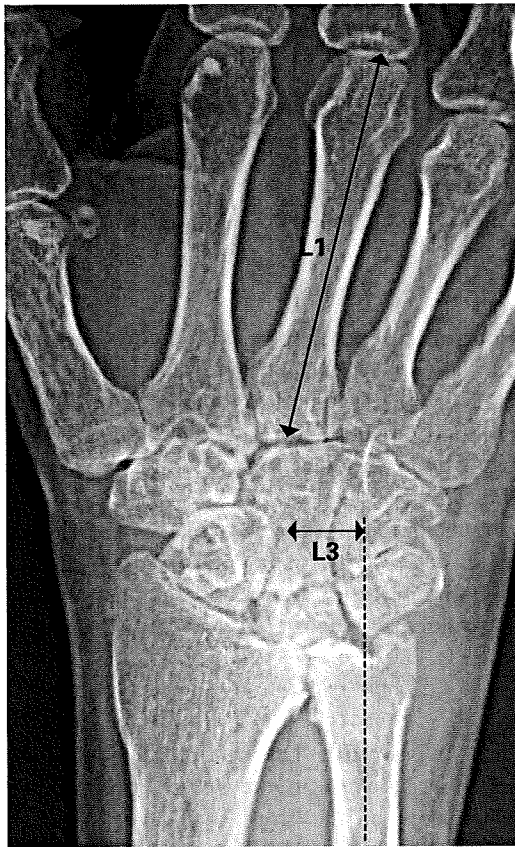


Fig. 1

Radiograph showing measurement of the carpal-ulnar distance ratio. It is calculated as $L3/L1$ where $L3$ is the distance between the centre of the capitate and the bony axis of the ulna and $L1$ the length of the third metacarpal. The normal ratio is 0.3 sd 0.03.

line perpendicular to the YZ plane and indicated palmar (+)/dorsal (-) displacement. Rotation around the Z axis produced flexion (+)/extension (-); that around the Y axis pronation (+)/supination (-) and that around the X axis indicated ulnar (+)/radial (-) deviation (Fig. 2). Thus, we calculated as a 3D vector the translocation of each carpal bone relative to the reference system determined for the radius.^{13,15}

Next, using the anatomical feature as described by Belsole et al¹⁴ the local co-ordinate system for the scaphoid, lunate, and capitate was established to characterise carpal direction (Fig. 3). The X axis of the scaphoid was defined as its principal axis, calculated as the line on which the moment of inertia was smallest and which ran through the centroid. The Z axis was defined as the line running through the dorsal ridge of the scaphoid in the plane perpendicular to the X axis and the Y axis was the line perpendicular to the XZ plane. The X axis of the lunate was defined as the line through the palmar and dorsal poles, the Y axis as the line through the centroid, perpendicular to the X axis and the Z axis as the line per-

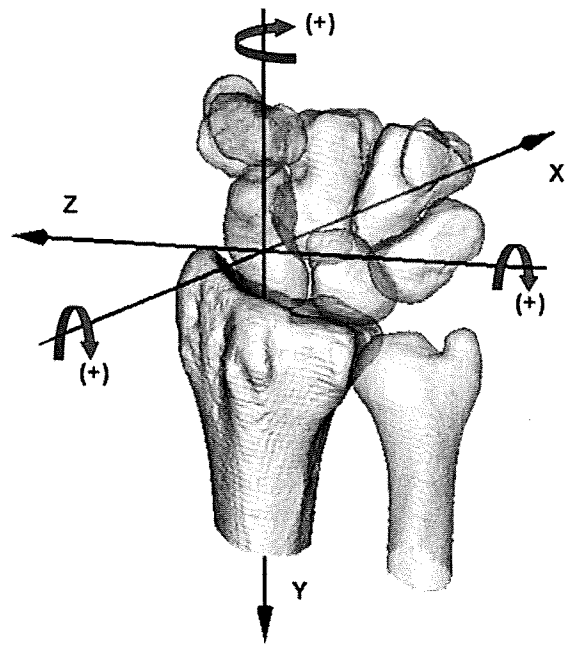


Fig. 2

A three-dimensional model showing details of the orthogonal reference system established in the radius as advocated by Belsole et al.¹⁵ The Y axis was the longitudinal radial axis and indicated the proximal (+)/distal (-) direction; the Z axis was the line through the styloid perpendicular to the Y axis and indicated radial (+)/ulnar (-) displacement; the X axis was the line perpendicular to the YZ plane and indicated palmar (+)/dorsal (-) displacement. Rotation around the Z axis produced flexion (+)/extension (-); that around the Y axis pronation (+)/supination (-) and that around the X axis indicated ulnar (+)/radial (-) deviation.

pendicular to the XY plane. The Y axis of the capitate was defined as its principal axis¹⁴ and the Z axis as the line through the dorsal joint ridge of the capitate-hamate joint perpendicular to the Y axis, rotated $+90^\circ$ around the Y axis. The X axis was the line perpendicular to the YZ plane. From these planes the 3D vector of a carpus relative to the radius was calculated with six degrees of freedom using the Euler angle¹² method. This quantified the direction and rotation of each carpal bone in the RA wrist relative to the radius and compared their positions with those of a normal wrist.

With regard to evaluating the translocation of location of the centroid, the variation in size of each carpal bone needed to be considered, and the translocation index was used for the purpose. It was calculated by dividing each of the three components of the vector of the centroids of the carpal bones by the square root of the cross-section of the radius at a plane perpendicular to its longitudinal axis and passing through Lister's tubercle¹⁶ (Fig. 4).

The translocation index was as follows:

$$(Tx, Ty, Tz) = x/\sqrt{S}, y/\sqrt{S}, z/\sqrt{S},$$

where x , y and z represent the vectors of the centroid of the carpal bone, relative to the origin of the reference of the

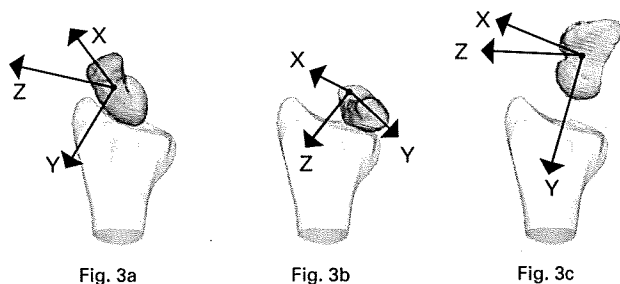


Fig. 3a

Fig. 3b

Fig. 3c

Diagram showing the orthogonal system as applied to a) the scaphoid, b) the lunate and c) the capitate according to Belsole et al.¹⁴ The X axis of the scaphoid was defined as its principal axis, calculated as the line on which the moment of inertia was smallest and which ran through the centroid. The Z axis was defined as the line running through the dorsal ridge of the scaphoid in the plane perpendicular to the X axis, and the Y axis as the line perpendicular to the XZ plane. The X axis of the lunate was defined as the line through the palmar and dorsal poles, the Y axis as the line through the centroid, perpendicular to the X axis, and the Z axis as the line perpendicular to the XY plane. The Y axis of the capitate was defined as its principal axis and the Z axis as the line through the dorsal joint ridge of the capitate-hamate joint perpendicular to the Y axis, rotated +90° around the Y axis. The X axis was the line perpendicular to the YZ plane.

radius (mm) and S was the cross-sectional area of the radius (mm²), at a plane perpendicular to its longitudinal axis at the level of Lister's tubercle (Fig. 4).

Statistical analysis. The left hand was converted to the orientation of the right hand and comparison of the results between the control and RA groups performed using standard statistical formulae based on the Mann-Whitney U-test. The results were deemed to be significant if $p \leq 0.05$.

Results

Centroid translocation. Three-dimensional images of the carpal bones showed that all centroids translocated not just in an ulnar direction, but also in the ulnar, proximal and volar direction, along the slope of the surface of the distal radius (Figs 5 and 6). Contacts between the radius and the scaphoid and the radius and the lunate were translocated ulnopalmarly and were incongruent in most cases. In the midcarpal joint, congruity was relatively well preserved compared with that of the radiocarpal joint in most cases (Fig. 7) while their radiographs showed joint narrowing (Fig. 1).

In the radioulnar deviation plane, the capitate ($p = 0.0011$), hamate, ($p = 0.0013$), lunate ($p < 0.0001$), scaphoid ($p = 0.0003$), triquetrum ($p < 0.0001$) and trapezoid ($p = 0.0197$), in RA wrists were significantly translocated to the ulnar side by a mean of 6.28, 4.68, 5.07, 7.10, 3.85 and 6.12 mm, respectively (Table I). In the flexion-extension plane all the centroids translocated in the palmar and proximal directions relative to the radius. The capitate ($p = 0.0083$), hamate ($p = 0.0037$) and scaphoid ($p = 0.0064$) in RA wrists were significantly translocated in the palmar direction by a mean of 3.21, 2.99 and 2.04 mm, respectively (Table I). The capitate ($p < 0.0001$), hamate

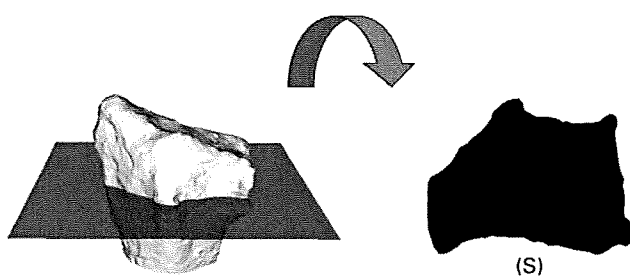


Fig. 4

Diagram showing the cross-section of the radius through Lister's tubercle, perpendicular to the longitudinal axis, S was the cross-sectional area of the radius (mm²).

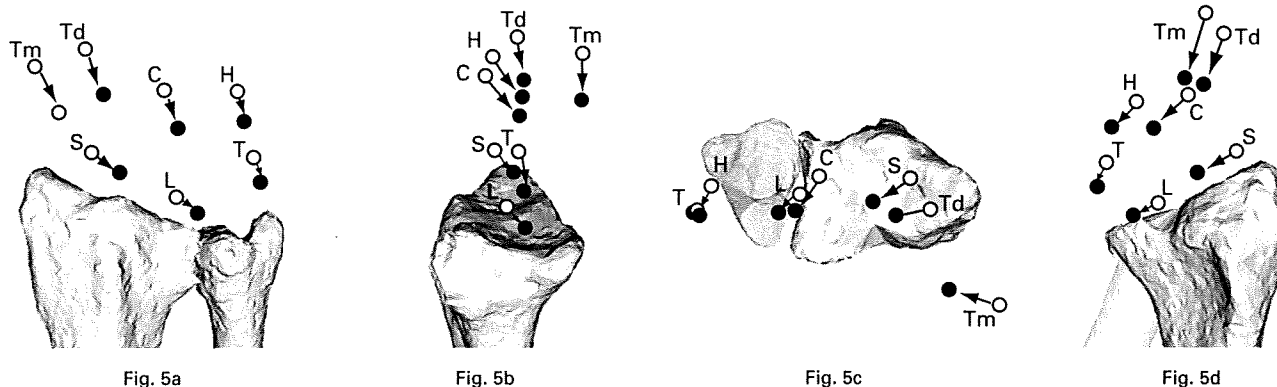
($p = 0.0037$), lunate ($p < 0.0001$), scaphoid ($p < 0.0001$) triquetrum ($p = 0.0011$), trapezium ($p < 0.0001$) and trapezoid ($p < 0.0001$) in RA wrists were significantly translocated proximally by a mean of 10.70, 9.41, 8.68, 6.90, 9.89, 11.37 and 13.30 mm, respectively (Table I).

Carpal rotation. The proximal row of RA wrists was flexed significantly compared with the normal wrists (Fig. 7b), the scaphoid at 25° ($p = 0.0003$) and the lunate at 10° ($p = 0.0311$) more than normal. In the pronation/supination plane, the scaphoid, lunate, and capitate did not supinate but were pronated 12°, 7° and 6°, respectively ($p = 0.053$, 0.147 and 0.356). The distal row was extended dorsally (Fig. 7c), as was the capitate by 12° ($p = 0.0387$) more than normal. The 3D images showed that the dorsally extended distal row corrected the hand to almost normal relative to the radius, by counteracting the flexion deformity of the proximal row.

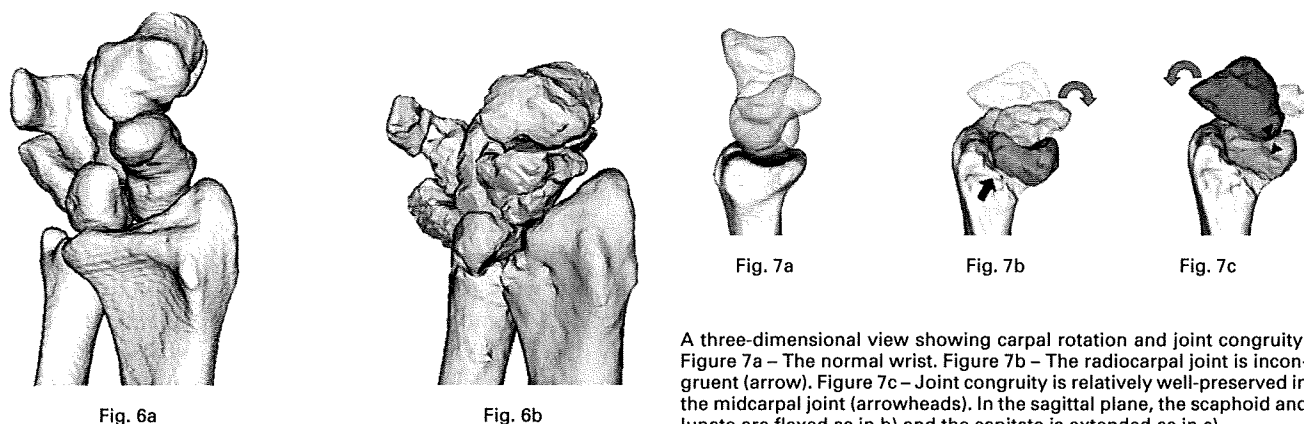
Discussion

In the RA wrist, ligamentous laxity is probably the major cause of collapse and instability.¹ There are many reports which have attempted to measure the deformity radiologically,^{2-4,6-8} but two-dimensional evaluation is of limited value. In our study, 3D imaging showed clearly that the rheumatoid carpus translocated obliquely in an ulnar, proximal and volar direction (Fig. 6). This quantitative technique allowed an easier understanding of this complex deformity. The direction of carpal translocation followed the natural slope of the joint surface of the distal radius which had a mean inclination of 24° in the coronal and 11° in the sagittal plane.^{16,17} In normal wrists, displacement of the carpus was resisted mainly by the palmar and dorsal radiotriquetral and palmar radiolunate ligaments.^{6,18,19} Their laxity probably allowed the 3D oblique translocation.

Rotational deformity, one of the most common deformities in RA, has been described qualitatively as carpal supination. Our 3D study, however, showed quantitatively that the main rotational deformity of the proximal row was



Diagrams showing centroid translocation from a) a dorsal view, b) ulnar view, c) distal view and d) radiopalmar view. All the centroids translocated in an ulnar, proximal and volar direction. The trapezium translated slightly in a dorsal direction according to the X component but, overall, translocated in a palmar direction (Tm, trapezium; Td, trapezoid; C, capitate; H, hamate; S, scaphoid; L, lunate; and T, triquetrum).



Three-dimensional radiopalmar view of the translation of the carpus in a) a normal wrist and b) rheumatoid arthritis. The carpus translocates along the direction of the slope of the joint surface of the distal radius.

A three-dimensional view showing carpal rotation and joint congruity. Figure 7a – The normal wrist. Figure 7b – The radiocarpal joint is incongruent (arrow). Figure 7c – Joint congruity is relatively well-preserved in the midcarpal joint (arrowheads). In the sagittal plane, the scaphoid and lunate are flexed as in b) and the capitate is extended as in c).

palmar flexion with no significant rotation. Accurate estimation of carpal supination by plain radiography may not be easy since palmar subluxation of the distal radius in relation to the ulna makes it difficult to obtain a true lateral view for measurement of carpal rotation in the transverse plane.

We also noticed a different pattern of rotational deformity between the radiocarpal and midcarpal joints. Our 3D study showed that the proximal row as flexed at the radiocarpal joint and the distal row extended at the midcarpal joint (Fig. 7). While flexion of the proximal row was associated with translocation, the extension of the distal row was associated only with minor translocation. Although our patients had joint narrowing throughout the carpus, the congruity and function of the midcarpal joint were better preserved even in deformed RA wrists than at the radiocarpal joint.

Moritomo et al²⁰ proposed a self-stabilising mechanism which is stronger in the midcarpal than in the radiocarpal

joint. A scaphoid under axial load against the trapezium tends to rotate in a flexion/ulnar direction. This turning effect is constrained by the extension/radial deviation moment of the triquetrum, leading to a stable equilibrium provided that the interosseous ligaments in the proximal row are intact. We speculated that, with loosening of many carpal ligaments, the radiocarpal joint may easily lose congruity. Whereas the deformity in this joint included translational and rotational elements, in the midcarpal joint the deformity was predominantly rotational. We considered the radiocarpal joint to be more incongruent and thereby more prone to cartilaginous damage.

Our study has limitations, the most important of which is that it was based on selected cases in which the whole carpal bones were shifted to the ulnar side, but the shapes were relatively recognisable on plain radiography. The other limitation was that age and gender were not fully matched between the RA and control wrists. It is possible that calculation of centroids and angles of rotation are influenced by erosion of the carpal bones with a subsequent alteration of shape. Our quantitative information,

Table I. Details of translocation in the carpal bones

Direction	Centroid translocation																				
	Capitate			Hamate			Lunate			Scaphoid			Triquetrum			Trapezium			Trapezoid		
	AD* (mm)	TI†	SD	AD (mm)	TI	SD	AD (mm)	TI	SD	AD (mm)	TI	SD	AD (mm)	TI	SD	AD (mm)	TI	SD	AD (mm)	TI	SD
Palmar																					
Normal	3.21	0.01	0.11	2.99	0.07	0.11	1.08	0.23	0.05	2.04	0.23	0.07	0.52	0.15	0.08	0.22	0.47	0.18	0.33	0.04	0.16
RA‡		0.17	0.16		0.22	0.21		0.33	0.18		0.37	0.16		0.20	0.21		0.54	0.16		0.07	0.17
Proximal																					
Normal	10.70	-0.57	0.14	9.41	-0.61	0.24	8.68	0.05	0.14	6.90	-0.20	0.06	9.89	-0.19	0.24	11.37	-0.83	0.16	13.30	-0.82	0.16
RA		-0.15	0.20		-0.26	0.20		0.48	0.27		0.10	0.15		0.25	0.27		-0.42	0.16		-0.32	0.17
Ulnar																					
Normal	6.28	0.19	0.19	4.68	0.70	0.19	5.07	0.35	0.09	7.10	-0.24	0.14	3.85	0.84	0.10	6.42	-0.49	0.26	6.12	-0.24	0.25
RA		0.52	0.18		1.04	0.23		0.66	0.14		0.05	0.14		1.17	0.16		-0.27	0.18		0.00	0.17


* AD, the absolute value of the difference of the mean translation (mm)

† TI, translocation index

‡ RA, rheumatoid arthritis

however, allowed early identification of the rheumatoid deformity and should be a guide to treatment, in particular in the decision as to whether to undertake radiocarpal fusion alone or to include the midcarpal joint.

Supplementary Material

 A further opinion by Dr Klemens Trieb is available with the electronic version of this article on our website at www.jbjs.org.uk

No benefits in any form have been received or will be received from a commercial party related directly or indirectly to the subject of this article.

References

1. Shapiro JS. The wrist in rheumatoid arthritis. *Hand Clin* 1996;12:477-98.
2. Kushner DM, Braunstein EM, Buckwalter KA, Krohn K, White HA. Carpal instability in rheumatoid arthritis. *Can Assoc Radiol J* 1993;44:291-5.
3. Muramatsu K, Ihara K, Tanaka H, Kawai S. Carpal instability in rheumatoid wrists. *Rheumatol Int* 2004;24:34-6.
4. Shapiro JS. A new factor in the etiology of the ulnar drift. *Clin Orthop* 1970;68:32-43.
5. Taleisnik J. Rheumatoid synovitis of the volar compartment of wrist joint: its radiological signs and its contribution to wrist and hand deformity. *J Hand Surg [Am]* 1979;4:526-35.
6. Flury MP, Herren DB, Simmen BR. Rheumatoid arthritis of the wrist: classification related to the natural course. *Clin Orthop* 1999;366:72-7.
7. Van Vught RM, van Jaarsveld CH, Hofman DM, Helders PJ, Bijlsma JW. Patterns of disease progression in the rheumatoid wrist: a long-term follow-up. *J Rheumatol* 1999;26:1467-73.
8. Shapiro JS. Wrist involvement in rheumatoid arthritis swan-neck deformity. *J Hand Surg [Am]* 1982;7:484-91.
9. Youm Y, McMurtry RY, Platt AE. Kinematics of the wrist: an experimental study of radial-ulnar deviation and flexion-extension. *J Bone Joint Surg [Am]* 1978;60-A:423-31.
10. Ochi T, Iwase R, Kimura T, et al. Effect of early synovectomy on the course of rheumatoid arthritis. *J Rheumatol* 1991;18:1794-8.
11. Lorensen WE, Cline HE. Marching cubes: a high resolution 3D surface construction algorithm. *Computer Graphics* 1987;21:163-9.
12. Goto A, Moritomo H, Murase T, et al. In vivo three-dimensional wrist motion analysis using magnetic resonance imaging and volume-based registration. *J Orthop Res* 2005;23:750-6.
13. Oka K, Moritomo H, Murase T, et al. Patterns of carpal deformity in scaphoid non-union: a 3-dimensional and quantitative analysis. *J Hand Surg [Am]* 2005;30:1136-44.
14. Belsole RJ, Hilbelink DR, Llewellyn JA, et al. Mathematical analysis of computed carpal models. *J Orthop Res* 1988;6:116-22.
15. Belsole RJ, Bilbelink DR, Llewellyn JA, Dale M, Ogden JA. Carpal orientation from computed reference axes. *J Hand Surg [Am]* 1991;16:82-90.
16. Palmer AK. Fractures of the distal radius. In: Green DP, ed. *Operative hand surgery*. Vol. 1. Third ed. New York: Churchill Livingstone, 1993:929-73.
17. Schuind FA, Linscheid RL, An KN, Chao EY. A normal data base of posteroanterior roentgenographic measurements of the wrist. *J Bone Joint Surg [Am]* 1992;74-A:1418-29.
18. Cooney WP, Garcia-Elias M, Dobyns JH. Anatomy of mechanics of carpal instability. *Surg Rounds Orthop* 1989;3:15-24.
19. Mizuseki T, Ikuta Y. The dorsal carpal ligament: their anatomy and function. *J Hand Surg [Br]* 1989;14:91-8.
20. Moritomo H, Murase T, Goto A, et al. In vivo three-dimensional kinematics of the midcarpal joint of the wrist. *J Bone Joint Surg [Am]* 2006;88-A:611-21.

Takashi Kitamura · Jun Hashimoto ·
Tsuyoshi Murase · Tetsuya Tomita · Takako Hattori ·
Hideki Yoshikawa · Kazuomi Sugamoto

Radiographic study of joint destruction patterns in the rheumatoid elbow

Received: 7 January 2006 / Revised: 1 April 2006 / Accepted: 3 April 2006 / Published online: 3 May 2006
© Clinical Rheumatology 2006

Abstract Knowledge of the pattern of joint destruction is important for planning the therapeutic approach to rheumatoid arthritis (RA) of the elbow. Accordingly, we carried out a large-scale radiographic study with the objective of elucidating the joint destruction pattern in rheumatoid elbows. From 2001 through 2003, we examined and took plain X-rays of both elbows of 193 RA patients (i.e., 386 elbows), consisting of 18 men and 175 women, with a mean age of 57.0 years. Radiographic images of the elbow joints were used to classify the degree of bone loss in various zones on the elbow joint surface into four grades of severity, and joint destruction was compared between the left and right elbows. In addition, correlation in the extent of bone loss between each of the zones of the same elbow and differences in the extent of bone loss were analyzed statistically. The results showed direct correlations for destruction of the elbow joint surface among the zones for the left and right elbow joints and in the same elbow joint. However, more severe destruction was observed on the radial side of the humeral trochlea, and it was surmised that destruction of the elbow joint must begin at that site and gradually spread mediolaterally. In addition, in the same elbow joint, the correlation in the degree of bone loss between the trochlea of humerus and the trochlear notch

was especially strong, indicating that the bone destruction at both sites represented mirror lesions. We conclude that when performing radiographic diagnosis of the joint damage in the rheumatoid elbow, knowledge of this pattern of joint destruction will be useful for assessing whether there is joint destruction in the initial stage and for deciding the therapeutic approach.

Keywords Elbow joint · Radiography · Rheumatoid arthritis

Introduction

The elbow joint is a common site for the development of rheumatoid arthritis (RA), and it is one of the most important joints in the upper limb as it controls the reach of the hand [1–4]. For this reason, disorders of the elbow joint can seriously interfere with activities of daily living (ADL) of RA patients. In general, when arthropathy is mild, therapy consists of conservative treatments such as drug administration and/or intraarticular injection of steroid. In severe disease, surgical treatments such as synovectomy and artificial elbow joint replacement may be performed [1–4]. For treatment selection and planning, it is very important for the physician to have a good understanding of the pattern of destruction that has occurred in the RA elbow joint. However, it is unfortunate that to date very few reports of analysis of the pattern of bone destruction in RA elbow joints have been published.

We therefore carried out a large-scale radiographic study with the objective of elucidating the pattern of RA elbow joint bone destruction.

Subjects

From 2001 to 2003, we examined plain X-rays of both elbow joints of 233 patients who satisfied the ARA diagnostic criteria. Forty of these patients were excluded from the present study due to previous synovectomy or

T. Kitamura (✉)
Department of Orthopedic Surgery, Kaizuka City Hospital,
3-10-20, Hori, Kaizuka,
Osaka 597-0015, Japan
e-mail: kitamura@tb3.so-net.ne.jp
Tel.: +81-0724-225865
Fax: +81-0724-396061

J. Hashimoto · T. Murase · T. Tomita ·
H. Yoshikawa · K. Sugamoto
Department of Orthopaedics,
Osaka University Medical School,
2-2, Yamadaoka, Suita,
Osaka 565-0871, Japan

T. Hattori
Department of Orthopedic Surgery, NTT West Osaka Hospital,
2-6-40, Karasugatsuji, Tennouji,
Osaka 543-8922, Japan

artificial elbow joint replacement (33 patients) or because the X-rays were unreadable (seven patients). The remaining 193 RA patients, i.e., 386 elbows, were the subjects of this study. They consisted of 18 men and 175 women, with an age range of 23~84 years (mean 57.0 years). History of drug administration, including steroids, and duration of RA were unclear.

Methods

Radiographic classification of the severity of RA was performed on the basis of plain X-ray anteroposterior images and lateral images of the bilateral elbow joints that were obtained for each patient at the time of final examination. X-rays were taken with the patient in a sitting position. Frontal views were obtained with the elbow joint extended and the forearm in the supine position, while lateral views were obtained with the elbow joint flexed at 90° and the forearm in the intermediate position. The frontal images were divided into three zones: the capitulum of the humerus (zone A), the radial side of the humeral trochlea (zone B), and the ulnar side of the humeral trochlea (zone C). The extent of destruction of the joint surface was determined for each of these zones. In addition, from the lateral view, the extent of joint surface destruction was determined for the olecranon (zone D).

Extent of joint destruction was assessed by reference to a template of the normal elbow joint that had been prepared in advance. The ratings used were grade 0, no bone loss; grade 1, less than 3 mm of bone loss from the joint surface; grade 2, bone loss of 3 to less than 6 mm; and grade 3, bone loss of 6 or more mm (Figs. 1 and 2).

We investigated the extent of bone destruction observed in each of the joint zones, and also investigated whether there was any correlation in destruction among the zones. In practice, we first investigated the correlation in the extent of bone loss in the same zone in both elbows of the same patient, and then compared joint destruction in the left and

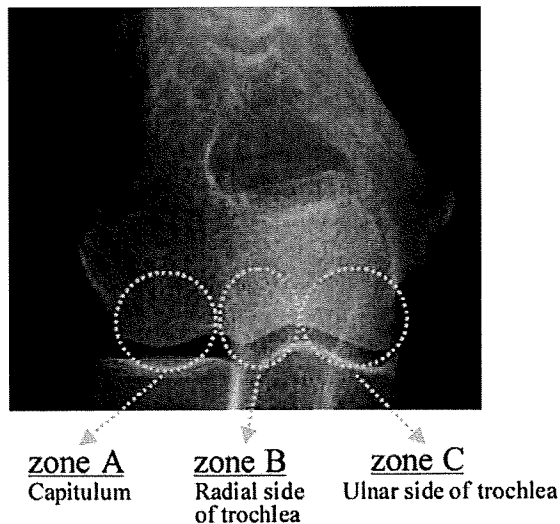


Fig. 1 Radiographic classification (zones A, B, and C)

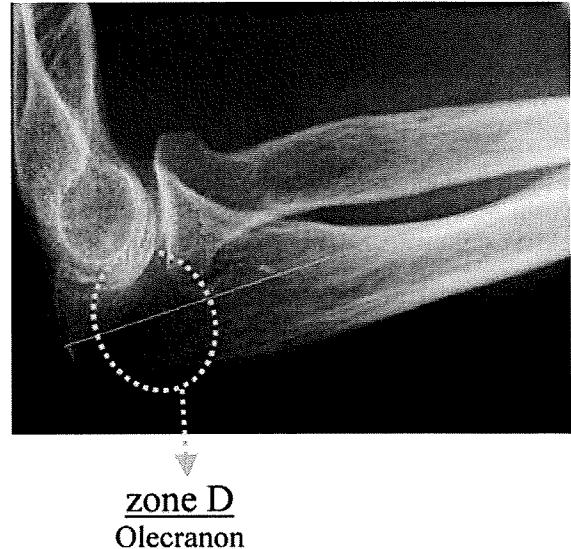


Fig. 2 Radiographic classification (zone D)

right elbows. In addition, the correlation in the extent of bone loss among each zone of the same elbow and differences in the extent of bone loss were analyzed statistically.

Spearman's ranked correlation coefficients were used for statistical analyses of correlations, while one-way analysis of variance (ANOVA) and Fisher's least significant difference (LSD) test were used to analyze differences in extent of bone loss.

Results

The extent of bone loss in each zone of the joint as seen on frontal X-ray images was as follows: zone A, 26.2% grade 0, 62.1% grade 1, 8.8% grade 2, and 2.8% grade 3; zone B, 26.2% grade 0, 37.0% grade 1, 26.9% grade 2, and 9.8% grade 3; and zone C, 26.9% grade 0, 62.1% grade 1, 2.6% grade 2, and 8.3% grade 3. The extent of bone loss was therefore similar in zone A and zone C, whereas zone B exhibited a lower percentage rated as grade 2 and a higher percentage rated as grade 3 compared with the other two zones. The extent of bone loss seen on lateral X-ray images (zone D) was grade 0 in 27.2%, grade 1 in 61.1%, grade 2 in 8.3%, and grade 3 in 3.4% (Table 1).

A significant correlation was found for the extent of bone loss in the same zone between the left and right elbows, and correlation was found for bilateral elbow joint destruction (zone A $r=0.833$, $p<0.001$; zone B $r=0.804$, $p<0.001$; zone C $r=0.881$, $p<0.001$; and zone D $r=0.887$, $p<0.001$).

In addition, statistically significant correlations were also found for the extent of bone loss among zones in the same elbow ($r=0.789\sim0.951$, $p<0.001$) (Fig. 3). A particularly strong correlation was demonstrated between zone C and zone D ($r=0.951$, $p<0.001$).

On the other hand, the extent of bone loss was significantly greater in zone B compared with zone A and zone C ($p<0.05$), indicating that joint surface

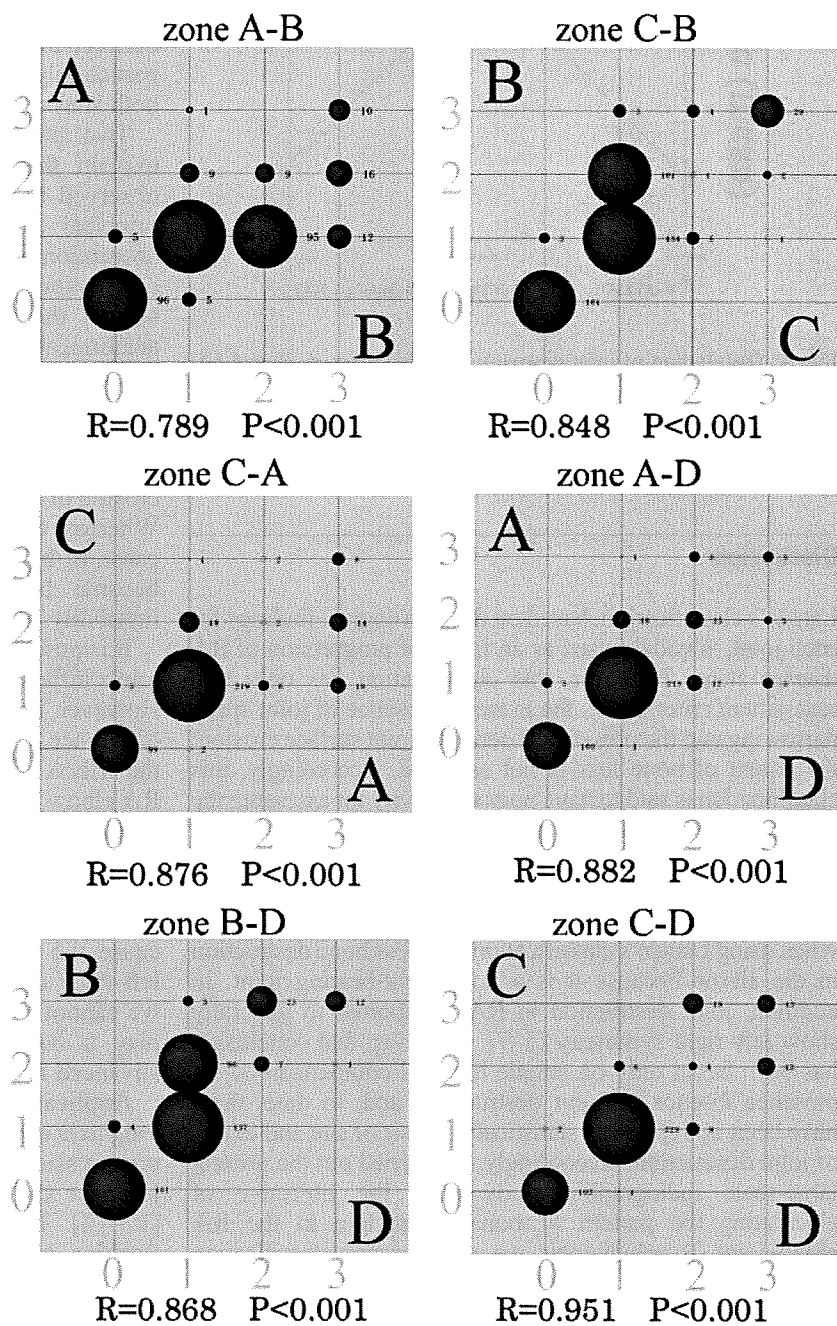
Table 1 Radiographic classification of severity of joint destruction in the elbow (*n*=193)

Grade	Zone A		Zone B		Zone C		Zone D	
	R/L	Total(%)	R/L	Total(%)	R/L	Total(%)	R/L	Total(%)
0	50/51	26.2	49/52	26.2	51/53	26.9	51/54	27.2
1	123/117	62.2	73/70	37.1	120/120	62.2	117/119	61.1
2	14/20	8.8	54/50	26.9	7/3	2.6	16/16	8.3
3	6/5	2.8	17/21	9.8	15/17	8.3	9/4	3.4
Total	193/193	100	193/193	100	193/193	100	193/193	100

destruction was more advanced in the central part of distal humerus articular surface than at other sites (Fig. 4).

In addition, bone destruction of the humeral trochlea that extended to the olecranon fossa, i.e., a so-called Y-shaped

Fig. 3 Correlation of joint destruction among zones A, B, C, and D (386 joints)



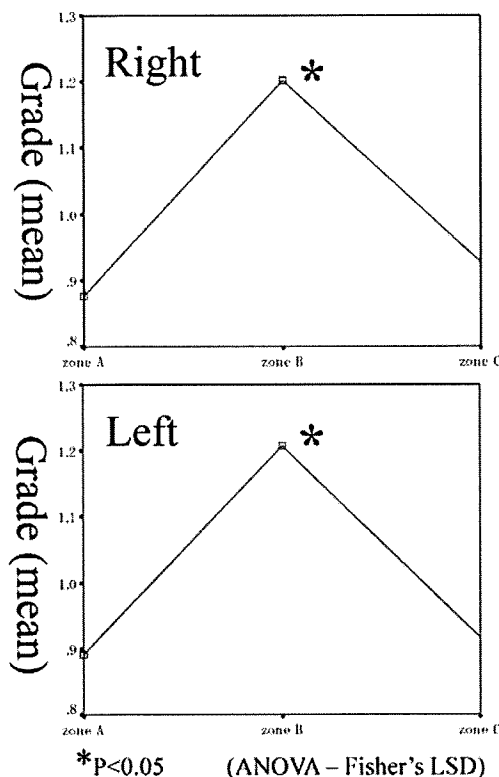


Fig. 4 Distribution of joint destruction grade (zones A, B, and C)

deformity, was observed in six of the patients, although this was bilateral in only two patients.

Discussion

Larsen's classification, based on the radiological findings for each joint, is widely used as an index of progression of RA disease stage. However, this classification has only two assessment criteria, i.e., the presence/absence of joint space narrowing and the presence/absence of joint surface erosion; the extent of bone loss is not assessed. Accordingly, this classification is said to have poor sensitivity for assessing the extent of joint destruction [5–7]. Lehtinen et al. [7] reported that joint space narrowing in the RA elbow differs from that in weight-bearing joints in that it occurs only subsequent to erosive destruction. They also stated that caution is necessary when using Larsen's classification to assess bone destruction in the elbow because it is a nonweight-bearing joint. In addition, joint destruction in RA is reported to generally show left–right symmetry [5–7]. However, that conclusion has been based only on simple bilateral comparison of the presence/absence of joint destruction, and, to date, there have been no reports of statistical analysis of site and extent of joint destruction. Accordingly, we carried out the present large-scale radiographic study with the objective of elucidating the pattern of bone destruction in the RA elbow joint. To achieve this, we used our own classification system to assess the extent of bone loss in various zones on the elbow joint surface, and joint destruction was compared

between the left and right elbows. We then performed statistical analyses to determine whether there were any correlations in the extent of bone loss among each of the zones in the bilateral elbows and in the same elbow.

Our patients showed positive correlations among each of the zones for the extent of bone loss in the same elbow joint, and positive correlations were also found for the extent of joint surface bone loss in the same zones in the bilateral elbows. On the other hand, when we investigated the extent of bone loss in each zone in the same joint, we found it to be significantly greater on the radial side of the humeral trochlea compared with the ulnar side of the trochlea and the capitulum. We therefore surmised that the joint destruction must begin at the radial side of the humeral trochlea and gradually spread mediolaterally. In addition, in the same elbow joint, the correlation in the degree of bone loss between the ulnar side of the trochlea and the olecranon was particularly strong, indicating that the bone destruction at both sites represented symmetrical lesions.

Two theories have been proposed in an attempt to explain the underlying mechanism of the destruction observed in upper limb joints with RA. In the first, the principal cause is considered to be destruction and absorption of cartilage and bone as a result of the actions of cytokines released from the synovial tissue [8, 9]. The second theory holds that the major effects arise from anatomical and/or mechanical factors [10]. Ochi et al. [11] reported that even in the same joint the mechanism of destruction varies widely depending on the disease type. That is, they found that in the type involving damage to the smaller joints, the main bone destruction consisted of erosion of the joint surface due to proliferation of synovitis. Whereas with the mutilating type of arthritis, the main cause of bone destruction was crushing of bone that had become highly osteoporotic because of severe joint instability due to joint laxity.

It is possible that the level of stress applied to the elbow joints differs between the dominant and nondominant arm. However, in the present study, we found no clear left–right difference in the extent of joint destruction, suggesting that the effects of mechanical factors on bone destruction in the RA elbow are slight. Even so, consideration must be given to the fact that most of the patients in our present series were at an earlier stage of the disease, showing a milder degree of joint destruction. Conversely, however, some patients with severe joint destruction, such as is likely to cause the so-called Y-shaped deformity, exhibited clear left–right differences in the extent of damage. Therefore, we cannot rule out the possibility that mechanical factors play a larger role than immunological factors in the advanced stages of joint destruction.

Application of axial compression in the direction of the long axis of the forearm reportedly results in almost equal transmission of the force to the radial joint and the ulnar joint, or slightly greater transmission to the radial joint [12–14]. The surface of the radial side of the humeral trochlea becomes the varus–valgus pivot point of the elbow [15], and for this reason it is possible that when joint laxity occurs due to synovitis, forces are concen-

trated in that area and this leads to the progression of joint destruction.

Our present results indicated the possibility that joint destruction in the RA elbow begins on the radial side of the humeral trochlea and gradually spreads mediolaterally. If we accept the validity of this pattern of destruction of the elbow joint, then when analyzing X-rays taken in the early stage of RA elbow joint damage, it should be possible to focus on the radial side of the humeral trochlea and determine whether joint destruction had already begun. In addition, if bone destruction on the radial side of the trochlea were mild, we would be able to conclude that the joint destruction was at an early stage and that a minimally invasive therapy such as synovectomy was indicated.

The progression of joint destruction can be considered influenced by various factors, such as medication (including NSAIDs, DMARDs, and steroids), disease duration, and progression of joint deformation due to aging or osteoporosis [16–19]. A limitation of the present study was that we were unable to discuss the possible effects of drug treatments, disease duration, and aging in our patient series. However, this is the first report of a statistical analysis of the pattern of joint destruction in the rheumatoid elbow, and we think that our findings will make a significant contribution to decision making regarding therapeutic approaches to RA of the elbow.

References

1. Boyd AD, Thornhill TS (1989) Surgical treatment of the elbow in rheumatoid arthritis. *Hand Clin* 5(4):645–655
2. Rosenberg GM, Tuner RH (1984) Nonconstrained total elbow arthroplasty. *Clin Orthop* 187:154–162
3. Linclau LA, Winia WPCA, Korst JK (1983) Synovectomy of the elbow in rheumatoid arthritis. *Acta Orthop Scand* 54 (6):935–937
4. Pritchard RW (1991) Total elbow joint arthroplasty in patients with rheumatoid arthritis. *Semin Arthritis Rheum* 21(1):24–29
5. Ljung P, Jonsson K, Rydgren L, Rydholm U (1995) The natural course of rheumatoid elbow arthritis: a radiographic and clinical five-year follow up. *J Orthop Rheumatol* 8:32–36
6. Lehtinen JT, Kaarela K, Kauppi MJ, Belt EA, Maenpaa HM, Lehto MUK (2002) Bone destruction patterns of the rheumatoid elbow: a radiographic assessment of 148 elbows at 15 years. *J Shoulder Elbow Surg* 11:253–258
7. Lehtinen JT, Kaarela K, Belt EA, Kauppi MJ, Skytta E, Kuusela PP, Kautiainen HJ, Lehto MUK (2001) Radiographic joint space in rheumatoid elbow joints. A 15-year prospective follow-up study in 74 patients. *Rheumatology* 40:1141–1145
8. Kirwan JR (1997) The relationship between synovitis and erosions in rheumatoid arthritis. *Br J Rheumatol* 36:225–228
9. Cuomo F, Greller MJ, Zuckerman JD (1998) The rheumatoid shoulder. *Rheum Dis Clin North Am* 24:67–82
10. Tan AL, Tanner SF, Conaghan PG, Radjenovic A, O'Connor P, Brown AK, Emery P, McGonagle D (2003) Role of metacarpophalangeal joint anatomic factors in the distribution of synovitis and bone erosion in early rheumatoid arthritis. *Arthritis Rheum* 48:1214–1222
11. Ochi T, Iwase R, Yonemasu K, Matsukawa M, Yoneda M, Yukioka M, Ono K (1988) Natural course of joint destruction and fluctuation of serum C1q levels in patients with arthritis. *Arthritis Rheum* 31:37–43
12. Amis AA, Dowson D, Wright V, Miller JH (1979) The derivation of the elbow joint forces and their relation to prosthesis design. *J Med Eng Technol* 3:229–234
13. Amis AA, Dowson D, Wright V (1980) Elbow joint force predictions for some strenuous isometric actions. *J Biomech* 13:765–775
14. Halls AA, Travill R (1964) Transmission of pressure across the elbow joint. *Anat Rec* 150:243–247
15. Morrey BF, An KN, Stormont TJ (1988) Force transmission through the radial head. *J Bone Jt Surg* 70-A:250–256
16. McIlwain HH (2003) Glucocorticoid-induced osteoporosis: pathogenesis, diagnosis, and management. *Prev Med* 36:243–249
17. Solomon DH, Levin Elaine, Helfgott SM (2000) Patterns of medication use before and after bone densitometry: factors associated with appropriate treatment. *J Rheumatol* 27:1496–1500
18. Minaur NJ, Kounail D, Vedi S, Compston JE, Beresford JN, Bhalla K (2002) Methotrexate in the treatment of rheumatoid arthritis. II. In vivo effects on bone mineral density. *Rheumatology* 41:741–749
19. Dolan AL, Moniz C, Abraha H, Pitt P (2002) Does active treatment of rheumatoid arthritis limit disease-associated bone loss? *Rheumatology* 41:1041–1047

Analysis of Radiocarpal and Midcarpal Motion in Stable and Unstable Rheumatoid Wrists Using 3-Dimensional Computed Tomography

Sayuri Arimitsu, MD, Kazuomi Sugamoto, MD, PhD, Jun Hashimoto, MD, PhD, Tsuyoshi Murase, MD, PhD, Hideki Yoshikawa, MD, PhD, Hisao Moritomo, MD, PhD

Purpose The kinematic evaluation of carpal motion, especially midcarpal motion, in rheumatoid arthritis (RA) has been extremely difficult because of limited imaging techniques previously available. The purpose of this study was to evaluate the amount of radiocarpal and midcarpal motion in the flexion-extension plane in both stable and unstable rheumatoid wrists using three-dimensional computed tomography.

Methods We acquired *in vivo* kinematic data on 30 wrists with RA by three-dimensional computed tomography with the wrist in 3 positions: neutral, maximum flexion, and maximum extension. All cases were radiographically classified into 1 of 2 subtypes, the stable form or unstable form, according to the classification by Flury et al. We evaluated the precise range of radiocarpal and midcarpal motion using a markerless bone registration technique and calculated the individual contributions to the total amount of wrist motion in the flexion-extension plane in the different radiographic subtypes of RA.

Results The average range of motion of radiocarpal and midcarpal joint was $27^\circ \pm 15$ and $32^\circ \pm 17$, respectively. The average contribution of midcarpal motion to the total amount of wrist motion was 54%. The average contribution of midcarpal motion in the unstable form was 67%, which was significantly higher than 47% ($p < .05$) in the stable form.

Conclusions Midcarpal motion of rheumatoid wrists in the flexion-extension plane was better preserved than previously thought. The contribution of midcarpal motion to the total amount of wrist motion was significantly greater ($p < .05$) in the unstable form than in the stable form of RA. (*J Hand Surg* 2008;33A:189–197. Copyright © 2008 by the American Society for Surgery of the Hand.)

Key words Kinematics, rheumatoid arthritis, three-dimensional, wrist.



THE INVOLVEMENT OF THE WRIST in rheumatoid arthritis (RA) is common, and surgical treatment is often required to alleviate persistent wrist pain. The natural course of destruction in a rheumatoid wrist has been

Department of Orthopaedic Surgery, Osaka University Graduate School of Medicine, Osaka, Japan.

The authors acknowledge the assistance during parts of the experimental procedure of Tetsuya Tomita, MD, PhD, Akira Goto, MD, PhD, Kunihiro Oka, MD, PhD, and Ryoji Nakao, Department of Orthopaedic Surgery, Osaka University Graduate School of Medicine.

Received for publication June 13, 2007; accepted in revised form November 15, 2007.

The authors received support from the Japan Science and Technology Agency.

Corresponding author: Sayuri Arimitsu, MD, Department of Orthopaedic Surgery, Osaka University Graduate School of Medicine, 2-2, Yamada-oka, Suita, Osaka 565-0871, Japan; e-mail: sayu@df6.so-net.ne.jp.

0363-5023/08/33A02-0007\$34.00/0
doi:10.1016/j.jhssa.2007.11.012

classified into 3 types by Simmen and Huber¹: type I, the ankylosis type; type II, the osteoarthritis type; and type III, the disintegrating type. Based on their radiologic analysis, type I has a spontaneous tendency to progress into ankylosis, type II resembles secondary osteoarthritic changes as destruction progresses, and type III has progressive destruction, loss of alignment, and finally complete collapse of the wrist.¹ In addition, Flury et al² proposed the classification of wrists with RA into a stable form of the disease (types I and II) and an unstable form of disease (type III) to make the choice and timing of surgical intervention easier (Table 1 and Fig. 1). It has generally been thought that the deterioration of midcarpal joint is more severe in the unstable form than in the stable form.³ Therefore, the partial arthrodesis technique, like radiolunate (RL) arthrodesis, has been applicable to the stable form, whereas the unstable form has been better treated by total arthrodesis of the wrist.³

Radiolunate arthrodesis is a well-established procedure for the RA wrists, and several researchers have reported the favorable clinical results of the procedure.²⁻¹² It has been suggested that RL arthrodesis is most useful in those

TABLE 1: Classification by the Natural Course of the Rheumatoid Wrist and the Radiologic Parameters Described by Simmen and Huber¹ and Flury et al²

	Classification		Radiologic Parameters	
	Simmen and Huber ¹	Flury et al ²	Ulnar Carpal Translocation* (mm)	Loss of Carpal Height Ratio*
Type I	Ankylosis	Stable form	3.7 (0–11)	Δ0.14 (0.01–0.28)
Type II	Osteoarthritis	Stable form	3.8 (0–8)	Δ0.16 (0.02–0.34)
Type III	Disintegration	Unstable form	9.5 (4–17)	Δ0.30 (0.10–0.46)

*The radiologic parameters 10 to 20 years after onset of RA represented by Simmen and Huber¹ (n = 126).

rheumatoid patients whose disease had left the midcarpal joints relatively unaffected as seen on the radiograph.¹ However, the preoperative evaluation of the midcarpal joint on the radiograph has been difficult because of the complicated and overlapping shapes of the carpal bones in RA deformities. Recently, researchers have been able to measure *in vivo* and three-dimensional (3-D) kinematics of the human joint using a markerless bone registration technique, which is a method for evaluating the precise motions by determining relative positions of bones in different volume images.^{13–19} We thought it would be possible to evaluate the kinematics of the carpal motion and quantify the midcarpal motion preoperatively in cases of RA with this 3-D technique.

The kinematic behavior of the carpal bones in rheumatoid wrist is not well-known, especially in relation to the RA subtypes. The purpose of this study was to evaluate the amount of radiocarpal and midcarpal motion in the flexion–extension plane in both stable and unstable rheumatoid wrists using 3-D computed tomography (3-D CT). We calculated the individual contributions of radiocarpal and midcarpal motion to the total amount of wrist motion to determine which radiographic subtype of

RA had the greater contribution of midcarpal motion to the total amount of wrist motion.

MATERIALS AND METHODS

Subjects

We randomly selected 30 wrists from 29 RA patients who were regularly treated with medication at our institution. All of them had pain and instability of the wrists. One patient was a man and 28 were women. The average age was 60 years (range, 21 to 80 years). The average duration of RA was 13 years (range, 6 to 38 years). For comparison, we investigated a control group of 10 normal wrists from 10 healthy volunteers comprising 8 men and 2 women whose average age was 29 years (range, 22 to 36 years). All subjects consented to be included in this study.

Radiographic Evaluation

To investigate the relationship between the contribution of midcarpal motion to the total amount of wrist motion and the radiographic appearance of RA, we classified 30 wrists with RA into 1 of the 2 subtypes, the stable form or the unstable form of the disease, by the natural course of the rheumatoid wrist and the radiologic parameters (Table 1 and

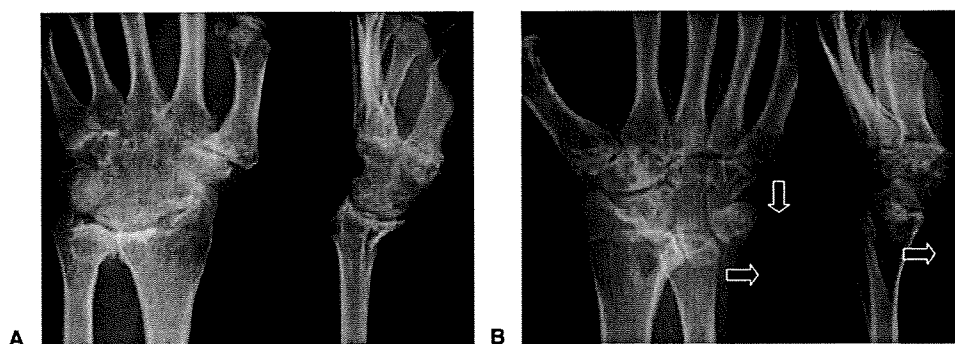


FIGURE 1: The **A** stable form and **B** unstable form of RA by the method of Flury et al.² **A** Representative case of the stable form of RA, which has a spontaneous tendency to progress into ankylosis (Video 1, a 3-dimensional animation of a representative case of the stable form of RA wrist, may be viewed at the *Journal's* Web site, www.jhandsurg.org). **B** Representative case of the unstable form of RA in which there is progressive destruction and loss of alignment. The carpal height is reduced and the carpal bones are dislocated ulno-palmarly with respect to the case shown in **A** (arrows) (Video 2, a 3-dimensional animation of a representative case of the unstable form of RA wrist, may be viewed at the *Journal's* Web site, www.jhandsurg.org).

Fig. 1).^{1,2} The radiographic parameters we used for classification were ulnar translocation and carpal height ratio (Table 1).¹ In the current study, we also investigated our cases with or without scaphoid-lunate (S-L) dissociation (the gap between scaphoid and lunate is more than 2 mm¹² on the anteroposterior radiograph) in relation to the radiographic subtypes of RA.

Image Acquisition

The technique we used for *in vivo* 3-D kinematic evaluation has been described in detail previously.¹⁴⁻¹⁹ For patients with RA, we performed 3-D CT on the wrists using a clinical helical type scanner with an image slice thickness of 0.625 mm (LightSpeed Ultra16; General Electric, Waukesha, WI). For the normal wrists of volunteers, magnetic resonance images were obtained using a 1.5-T commercial magnetic resonance imaging (MRI) system (Magnetom Vision PlusR 1.5T MRI; Siemens, Munich, Germany) in conjunction with a receive-only surface coil of 2.3 ms/33 ms, a flip angle of 45°, a 160-mm field of view, and 0.5-mm-thick contiguous slices, with 0.6 × 0.8 mm pixels. For each wrist, we acquired image with the wrist in 3 different positions: neutral (in which the third metacarpal and the forearm axis were aligned), maximum wrist flexion, and maximum wrist extension. For normal volunteers, we used a custom-made device to hold the position during image acquisition. However, we could not use the device for RA patients because of pain and deformity of the wrists. Data were saved in a standard format (Digital Imaging and Communications in Medicine [DICOM]) that is used commonly for transferring and storing medical images.

Segmentation and Construction of a 3-D Surface Bone Model

Segmentation was defined as extracting bone regions individually. The anatomic structure or region of interest must be delineated and separated so that it can be viewed individually and 3-D bone models can be reconstructed. Regions of individual bones were segmented semiautomatically using a software program for image analysis (Virtual Place-M; AZE, Ltd., Tokyo, Japan). The software generated 3-D surface bone models using the marching cubes technique.^{14,15,20}

Registration

We created 3-D bone models and quantitatively evaluated the motion of the midcarpal joint using a markerless volume-based registration technique. The kinematic variables were calculated by registering the bone, obtained by segmentation, from one position to another. The accuracy of volume-based registration has been discussed previously,^{14,15} the mean rotation error was 1° ± 1, and the mean translation error was 0.21 mm ± 0.25.

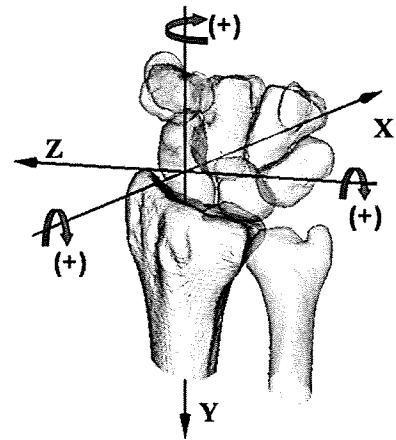


FIGURE 2: A consistent orthogonal reference system established in the radius.

Three-Dimensional Quantification of the Range of Motion

To quantify the 3-D range of motion of the midcarpal joint, we defined the grid for the radius, which was the orthogonal reference system advocated by Belsole et al (Fig. 2).^{15,21,22} The total amount of wrist motion in the flexion-extension plane was defined as the total range of motion of the radiocarpal and midcarpal joint in the flexion-extension plane, which was evaluated by assessing the range of capitate motion relative to the reference system established on the radius. The range of radiocarpal motion in the flexion-extension plane was investigated by that of the lunate motion. Then the range of the midcarpal motion in the flexion-extension plane could be quantified as the difference between the total amount of wrist motion and the range of radiocarpal motion.

In the flexion-extension motion of the wrist, the radiocarpal and midcarpal joints have motions in planes other than the flexion-extension plane such as the pronation/supination (P/S) plane and the radial/ulnar deviation (RD/UD) plane. There are coupling motions associated with wrist motion in the flexion-extension plane. We defined the 2 motions in the other planes as *out of the plane motion (P/S)* and *out of the plane motion (RD/UD)*, respectively. We quantified the amount of wrist motion in the flexion-extension plane and out of the plane separately for the radiocarpal and midcarpal joints.

A consistent orthogonal reference system was established in the radius as follows.²² The y axis was defined as the longitudinal radial axis and indicated the proximal (+)/distal (-) direction. The z axis was defined as the line running through the styloid process on the plane perpendicular to the y axis and indicated the radial (+)/ulnar (-) direction. The x axis was defined as the line perpendicular to the yz plane and indicated the palmar (+)/dorsal (-) direction. Rotation around the z axis produced flexion (+)/extension (-), rotation around the y axis was pronation (+)/supination (-), and rotation around the x axis was ulnar (+)/radial (-)